

High-temperature mobility of pure *n*-type InP epitaxial layers

M. Benzaquen, D. Walsh, and K. Mazuruk

Department of Physics, McGill University, 3600 University Street, Montreal, PQ, Canada H3A-2T8

(Received 18 March 1987)

High-purity epitaxial *n*-type InP thin layers give usually a reduced room-temperature Hall mobility compared to both bulk material and theoretical expectations. This effect occurs despite high low-temperature mobility, and is interpreted as due to a residual deep-donor center which acts as a strong scatterer and provides the additional electronic excitation observed at high *T*. A binding energy of 160 meV is found to be consistent with both the free-electron concentration and the computed Hall mobility.

At room temperature, the electron mobility in III-V epitaxial compounds is often observed to be lower than the theoretical predictions based on well-established physical parameters. In early GaAs epitaxial layers this was often the case for heavily compensated material. This effect has been explained, for moderately doped GaAs samples, by the presence of an isoelectronic acceptorlike complex related to carbon.¹ Such a center acts as a very strong scatterer, the corresponding scattering mechanism being important in the whole *T* range, and dominant at room temperature.² A similar problem appears for *n*-type InP epitaxial material, generally grown by metal-organic vapor-phase epitaxy (MOVPE), for which the room-temperature Hall mobility often falls below the theoretical results.^{3,4,5} This has led to various reassessments of the acoustical deformation potential E_1 , the values quoted in the literature ranging from 3.4 to 21 eV.^{6,7} Those values are generally obtained by fitting high-*T* Hall-mobility experimental results to a theoretical model accounting for a single shallow-donor species by including the appropriate scattering mechanisms. Such a procedure is only suitable if particular care is exercised. It is not applicable if additional scatterers are present or if impurity conduction is significant. A more reliable way of determining E_1 is the fit of an appropriate theoretical model including the usual scattering mechanisms to the Hall mobility μ_H in the whole *T* range, for samples well below the Mott limit to avoid impurity conduction effects,⁸ while keeping consistency with the variations of the Hall electronic concentration n_H as a function of *T*.^{9,10} This is due to the fact that increasing E_1 to obtain agreement with a low μ_H at 300 K also decreases very significantly the corresponding 78 K value, which cannot then be fitted unless unrealistically low values of N_{D1} , the shallow donor concentration, and N_A , the acceptor concentration, are assumed. Nevertheless, the value $E_1 = 6.8$ eV often quoted^{11,12} gives excellent agreement with a set of experimental results in a broad *T* range^{9,10} and has been obtained independently of electrical transport measurements.¹³ Moreover, the maximum room-*T* theoretical Hall mobility, found to be slightly above $6000 \text{ cm}^2 \text{ V}^{-1} \text{ s}^{-1}$ by using $E_1 = 6.8$ eV,^{10,11} is now more easily approached⁶ as the purity of the layers improves. If good agreement cannot be obtained between theory and experiment with a reasonable choice of E_1 ,

N_{D1} , and N_A , this may indicate the presence of some additional scattering mechanism.

We report on a set of three *n*-type InP samples grown by metal-organic vapor-phase epitaxy (MOVPE). The samples are pure enough to avoid impurity conduction effects except at the very lowest *T*.^{14,15} All samples are a few μm thick and have good uniformity.

Hall transport measurements have been performed on all three InP samples under low electric and magnetic field conditions using a high-impedance automated data acquisition system from 4.2 to 300 K. A standard bridge configuration was used. To avoid gradient effects, the temperature *T* recovered naturally from its lowest value at a very slow rate. In order to maintain the low electric field regime, the excitation current through the samples needed frequent adjustments. Low magnetic field conditions were preserved by using a 2-kG field at intermediate temperatures, where the mobility peaks,¹⁶ and 5 kG elsewhere.

Figure 1 shows the behavior of μ_H versus *T* for sample 3. The corresponding 77- and 300-K Hall mobilities quoted in Table I show reasonable agreement with available theoretical tables,¹⁰ thus suggesting a normal behavior for this sample. Figure 2 shows the corresponding variations as a function of *T* of the Hall electronic concen-

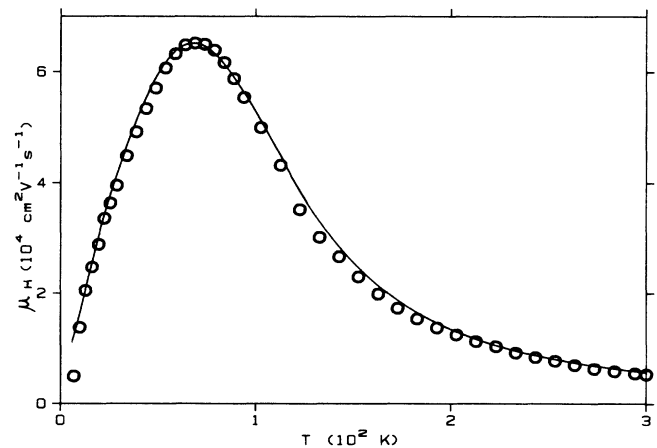


FIG. 1. μ_H vs *T* for sample 3. The continuous line is the Hall mobility computed with the parameters given in Table I.

TABLE I. Results obtained from the analysis of three InP samples. N_{D1} , N_{D2} , and N_A are, respectively, the shallow, deep-donor, and acceptor concentrations; $\mu_{HE}^{300\text{ K}}$ is the experimental Hall mobility at 300 K, $\mu_{HT}^{300\text{ K}}$ and $(\mu_{HT}^{300\text{ K}})'$ being the corresponding theoretical results when the deep center is and is not accounted for, respectively; n_{HE} , $n_{HT}^{300\text{ K}}$, and $(n_{HT}^{300\text{ K}})'$ are the corresponding Hall electronic concentrations at the given temperatures; E_{D2} is the binding energy of the deep center with degeneracy factor β and effective radius a .

Sample no.	N_{D1} (cm ⁻³)	N_{D2} (cm ⁻³)	N_A (cm ⁻³)	$\mu_{HE}^{300\text{ K}}$	$\mu_{HT}^{300\text{ K}}$ (cm ² V ⁻¹ s ⁻¹)	$(\mu_{HT}^{300\text{ K}})'$	$n_{HE}^{77\text{ K}}$ (cm ⁻³)
1	9.10×10^{14}	1.15×10^{14}	7.35×10^{14}	4060	4135	5785	1.32×10^{14}
2	1.59×10^{15}	8.20×10^{13}	1.18×10^{15}	4890	4934	5620	2.93×10^{14}
3	1.98×10^{15}	0.0	1.04×10^{15}	5260		5628	6.40×10^{14}

Sample no.	E_{D2} (meV)	a (Å)	β	$n_{HE}^{300\text{ K}}$ (cm ⁻³)	$n_{HT}^{300\text{ K}}$ (cm ⁻³)	$(n_{HT}^{300\text{ K}})'$ (cm ⁻³)
1	160	1300	1.2	2.19×10^{14}	2.20×10^{14}	1.43×10^{14}
2	160	1000	1.5	3.76×10^{14}	3.83×10^{14}	3.37×10^{14}
3			0.8	7.60×10^{14}		7.69×10^{14}

tration defined as

$$n_H = n_c / r_H, \quad (1)$$

n_c being the electronic concentration in the conduction band and r_H the Hall factor.

Figures 3 and 4 present μ_H as a function of T , respectively, for samples 1 and 2. The corresponding room- T experimental Hall mobilities are reported in Table I, and appear too low for the corresponding values at 77 K.¹⁰ Figures 5 and 6 show, respectively, the corresponding variations of n_H as a function of T . This behavior is clearly different from sample 3, as can also be seen from the values of n_H quoted in Table I, corresponding to 77 and 300 K. For sample 3, n_H stabilizes above 100 K as most of the shallow donors become ionized. This is not the case for the two other samples studied here, where, after a similar stabilization around 100 K, additional electron excitation is observed above 200 K. This effect has been recently reported,¹⁷ and is interpreted as being due to the presence of an additional donor center which is neutral at low T and starts to ionize when the temperature is increased and the Fermi level falls deeper in the forbidden gap. This interpretation is supported by some

photoluminescence data.¹⁷ We then speculate that this behavior corresponds to the presence of a deep center or complex, whose origin is still unclear, with a concentration denoted as N_{D2} . Moreover, we point out that this additional electronic excitation is accompanied by a reduction in the Hall mobility which is more pronounced when the excitation becomes stronger. This appears clearly from the experimental data: sample 1, which has the highest low- T mobility, shows also both the largest high- T electronic excitation to the conduction band and the lowest room- T mobility (Figs. 5 and 3, respectively); for sample 2, both the reduction in mobility and the electronic excitation appear clearly, but are weaker; sample 3 does not show high- T excitation, and both the 77- and 300-K Hall mobilities are consistent, with reasonable precision, with theoretical predictions.¹⁰ The experimental results described above are not only representative of a fairly large number of samples tested by us, but also of most of the results recently quoted in the literature.³⁻⁵ All this

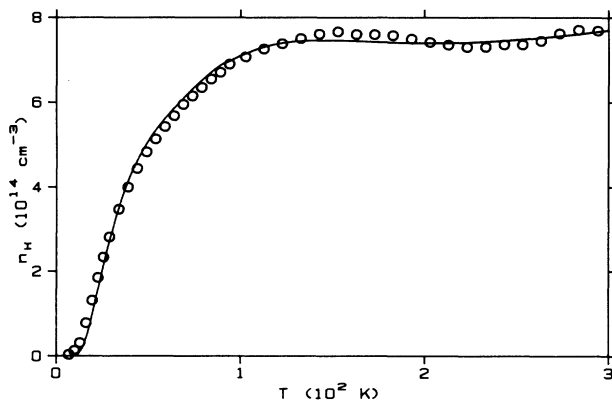


FIG. 2. n_H vs T for sample 3. The continuous line is the Hall electronic concentration computed with the parameters given in Table I.

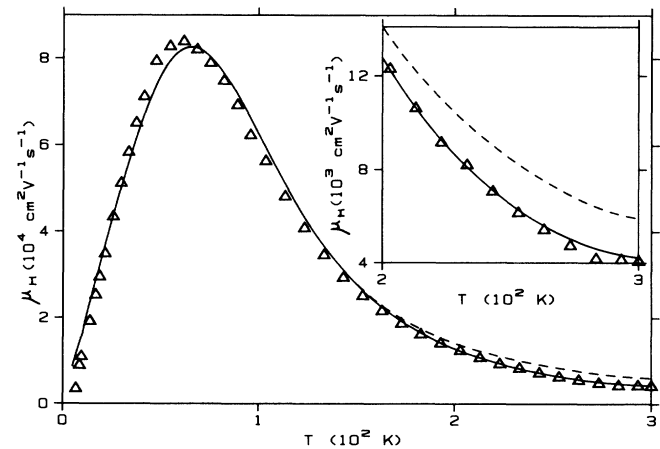


FIG. 3. μ_H vs T for sample 1. The continuous lines represent the computed Hall mobilities when the effects of a deep center are included with the parameters given in Table I. The dashed lines correspond to the same parameters but when only a single shallow donor is considered.

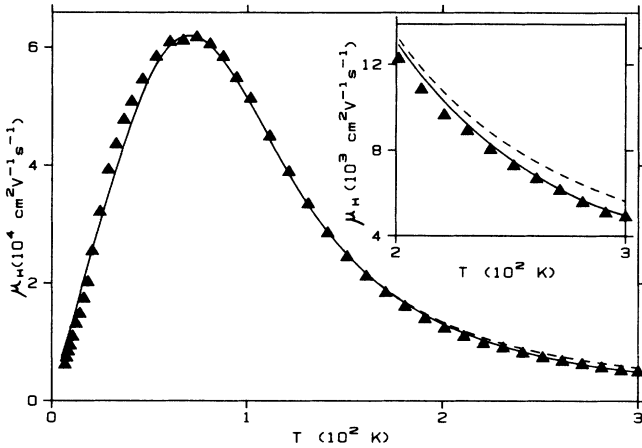


FIG. 4. μ_H vs T for sample 2. The continuous lines correspond to the Hall mobility computed with the parameters of Table I. The dashed lines correspond to the same parameters when the effect of the deep center is excluded.

indicates that the reduced Hall mobility and the electronic excitation are closely linked. Consequently, a simple interpretation of the results is that the deep centers act as strong additional scatterers as they become ionized. The different electric properties of sample 3 are only obtained occasionally and appear to be linked to trimethylindium, a source material used for the growth. When the room- T mobility of a sample is high, the 77-K mobility is comparatively low and inversely. Such effects seem to be a reflection of the variations of the ratio of deep to shallow impurity concentrations contained in this chemical.

To fit the electrical transport results of sample 3, for which a standard behavior is expected, μ_H is computed by an iterative solution to the Boltzmann equation due to Rode¹¹ without having to assume Matthiessen's rule. Ionized impurity scattering has been accounted for by the Brooks-Herring relaxation time,¹⁸ the other elastic scatter-

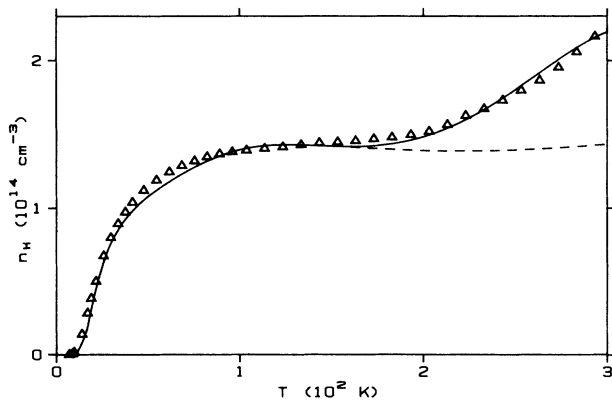


FIG. 5. n_H vs T for sample 1. The continuous lines are the Hall electronic concentration calculated with the parameters given in Table I, with excitation from a deep level. The dashed lines correspond to the same parameters but with a single shallow donor.

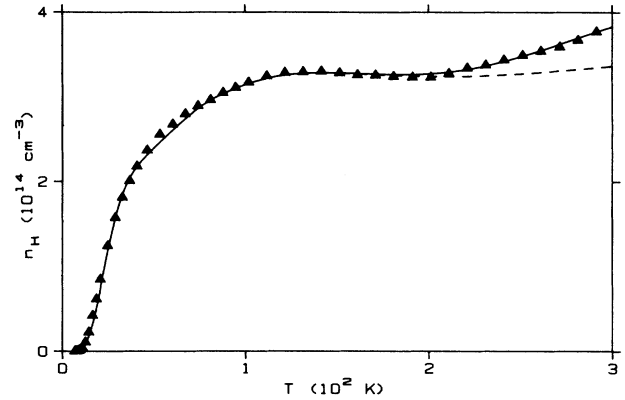


FIG. 6. μ_H vs T for sample 2. The continuous line is the Hall electronic concentration calculated with the parameters given in Table I. The dashed lines correspond to the same parameters, with the exclusion of the deep center.

ing mechanisms included being deformation-potential acoustic and screened piezoelectric.¹⁹ The small neutral impurity scattering has been neglected. The Rode iterative technique accounts then for polar optical scattering and has been applied in the form that does not account for nonparabolicity corrections in the conduction band. The computation requires the value of n_c and of the Fermi level E_F , which are related to the impurity concentrations N_{D1} and N_A and to the binding energy E_D through the neutrality equation. In our case, degenerate statistics were used for a single donor level with degeneracy factor β . This is justified at very low temperatures when the Fermi level lies, depending on compensation, close enough to the conduction-band edge to cause failure of the Boltzmann approximation. The values of N_{D1} , N_A , and E_D allow then the computation of $g(E)$, the perturbation to the equilibrium distribution function. $g(E)$ defines a pseudo-relaxation-time $\tau(E)$, which in turn allows the calculation of r_H and of the drift mobility by using the usual averaging integrals. n_c being given by the neutrality equation, n_H can also be calculated by using the computed values of r_H . Table II shows the values of the physical parameters of InP used in the computation.^{11,12} m^* is the relative effective mass, ϵ_s and ϵ_∞ the static and high-frequency dielectric constants, respectively, T_{PO} the Debye temperature, ρ_m the mass density, E_1 the acoustical deformation potential, C_L the longitudinal speed of sound, and P a dimensionless piezoelectric coefficient

TABLE II. Physical parameters of InP used in the computation.

m^* (a.u.)	0.082
ϵ_s	12.38
ϵ_∞	9.55
T_{PO} (K)	497
ρ_m (g/cm ³)	4.487
E_1 (eV)	6.8
C_L (cm/s)	5.028×10^5
P	0.013

defined by Hutson.¹⁹ The average binding energy for InP was taken as 6 meV. The parameters of the fit are N_{D1} and N_A , with initially $\beta = \frac{1}{2}$.

The continuous lines of Figs. 1 and 2 are the results of the previous calculation when applied to sample 3. The fit is in good agreement with the experimental results and was obtained in the following way. Values for N_{D1} and N_A at 300 K were first estimated, where

$$n_C^{300\text{ K}} = N_{D1} - N_A \quad (2)$$

holds for pure enough material, as in such a case almost all shallow donors are ionized at room temperature.⁹ $n_C^{300\text{ K}}$ is the electronic concentration in the conduction band at 300 K. The difference $N_{D1} - N_A$ was varied at 300 K until good agreement was obtained with the corresponding experimental value of n_H . This difference was then kept constant by varying both N_{D1} and N_A to obtain consistency with the experimental Hall mobility at 77 K. μ_H and n_H were then computed with the resulting values of N_{D1} and N_A for 50 points in the whole temperature range. For each temperature, 401 values of the total relaxation time were computed with a precision of 1% of the Rode iterative technique.¹¹ Below 50 K, $\beta = \frac{1}{2}$ gave a theoretical n_H approximately 20% lower than the observed values. This discrepancy disappeared with the value of β quoted in Table I. This value is larger than the expected one and could be attributed to the random distribution of the impurities, which in fact gives rise to an impurity band of totally localized states¹⁴ and not to a single discrete level. A correction for possible depletion effects in the epilayers not only was not necessary, but further increased the discrepancy observed for n_H at low T with $\beta = \frac{1}{2}$.

The previous approach is not sufficient to explain the behavior of samples 1 and 2. We then assume the presence of a deep-donor center with binding energy E_{D2} and concentration N_{D2} . The neutrality equation now becomes

$$n_C = N_{D1}^+ + N_{D2}^+ - N_A, \quad (3)$$

where the superscript + denotes the ionized donors. Moreover, we suppose that when these centers ionize, they are able to scatter the free electrons. The simplest choice for a scattering potential is a square well of the form

$$V(r) = \begin{cases} v_0, & r < a \\ 0, & r > a \end{cases} \quad (4)$$

V_0 is negative and corresponds to the depth of the well, a being the corresponding radius. For a deep center, the scattering potential is generally larger than the energy of the incident particles. This potential cannot then be considered as a small perturbation to the energy of the electrons, and the Born approximation is not valid to calculate the corresponding scattering cross section. A phase-shift calculation is thus necessary. Sclar²⁰ related the successive phase shifts δ_L to the relaxation time τ_1 through the general expression

$$\frac{1}{\tau_1} = \frac{4N_{D2}^+ \hbar}{m^* k} \sum_{L=0}^{\infty} (L+1) \sin^2(\delta_L - \delta_{L+1}), \quad (5)$$

where \hbar is the Planck constant divided by 2π , k the modulus of the wave vector of the incident electron, and m^* its effective mass. The concentration of scattering centers has been taken as N_{D2}^+ . For the potential of Eq. (4), the phase shifts are given by^{20,21}

$$\tan(\delta_L) = \frac{kj'_L(ka) - \gamma_L(\alpha, a)j_L(ka)}{kn'_L(ka) - \gamma_L(\alpha, a)n_L(ka)}, \quad (6)$$

where j_L and n_L are, respectively, the spherical Bessel and Neuman functions; j'_L and n'_L are the corresponding derivatives and

$$\gamma_L(\alpha, a) = \alpha j'_L(\alpha a) / j_L(\alpha a), \quad (7)$$

with

$$\alpha = [2m^*(E - V_0)]^{1/2} / \hbar,$$

E being the energy of the incident electron.

Equations (6) and (7) allow the analytical calculation of the phase shifts at any order, but this is unpractical and extremely tedious except for the first few.²⁰ It is nevertheless necessary when ka is of the order of one or greater.²⁰ For such a situation, an iterative procedure, suitable for a numerical calculation, can be used to compute τ_1 in Eq. (5).

By using the recurrent properties of the spherical Bessel and Neuman functions and their derivatives, Eqs. (6) and (7) can be rewritten, respectively, as

$$\tan(\delta_L) = \frac{j_{L-1}(ka) - j_L(ka) \left[\frac{L+1}{ka} + \frac{\gamma_L(\alpha, a)}{k} \right]}{n_{L-1}(ka) - n_L(ka) \left[\frac{L+1}{ka} + \frac{\gamma_L(\alpha, a)}{k} \right]}, \quad (8)$$

$$\gamma_L(\alpha, a) = \frac{\alpha^2}{\frac{L-1}{a} - \gamma_{L-1}(\alpha, a)} - \frac{L+1}{a}, \quad (9)$$

with

$$j_L(ka) = \frac{2L-1}{ka} j_{L-1}(ka) - j_{L-2}(ka), \quad (10)$$

the same expression being valid for $n_L(ka)$.

To initialize an iterative procedure for given k , V_0 , and a , the knowledge of $\gamma_0(\alpha, a)$, δ_0 , and δ_1 is required (quoted by Sclar²⁰). j_0 , j_1 , n_0 , and n_1 being well-known functions, the phase shifts can then be easily calculated to any order by using sequentially Eqs. (10), (9), and (8). The relaxation time of Eq. (5) is then a function of E , V_0 , and a . V_0 and a are additional parameters for the computation. In practice, iterations were halted when the relative variation between successive phase shifts fell below 10^{-6} . This yielded values of a few units for L at low energy, and of more than 100 at high energy.

When the effects of this additional center are added to the previous computation through the neutrality equation [Eq. (3)] and the inclusion of the relaxation time of Eq. (5), the model requires the five parameters N_{D1} , N_{D2} , N_A , E_{D2} , and a , with the assumption that the depth of the well corresponds to the binding energy. The degeneracy factor of the deep level is taken as $\frac{1}{2}$.

To fit this model to the experimental results for samples 1 and 2, the following procedure was used. As the deep center is not expected to have any effect in both n_H and μ_H at low T , it was not accounted for in a first step. n_H was then computed at 120 K—where most of the shallow donors are already ionized and the deep ones still neutral—by varying the difference $N_{D1}-N_A$ until good agreement was obtained with the corresponding measured value. N_{D1} and N_A were then varied in a way such that the difference $N_{D1}-N_A$ was maintained constant to get consistency with the measured Hall mobility at 77 K. As for sample 3, a value of β larger than $\frac{1}{2}$ corrected a similar discrepancy in n_H at low T . This yielded the final values of N_{D1} , N_A , and β quoted in Table I. In a second step, the binding energy E_{D2} was varied with rough estimates of N_{D2} and a until the start of the observed additional electronic excitation (Figs. 4 and 6) was reproduced by the model. The exact value of N_{D2} controls the amount of electronic excitation at 300 K and is then determined from the experimental room- T value of n_H . Finally, the value of the radius a of the well is obtained by fitting the room- T Hall mobilities. The parameters resulting from the fit are quoted in Table I, where $\mu_{HE}^{300\text{ K}}$ and $\mu_{HT}^{300\text{ K}}$ are, respectively, the experimental and theoretical Hall mobilities at room T , in very good agreement. $n_{HE}^{77\text{ K}}$ and $n_{HE}^{300\text{ K}}$ are the experimental values of n_H at 77 and 300 K, respectively. $(\mu_{HE}^{300\text{ K}})'$ and $n^{(300\text{ K})}'$ are the corresponding theoretical results when $N_{D2}=0$. The continuous lines of Figs. 3–6 were obtained with the parameters of Table I by including the deep centers in the calculation. The dashed lines correspond to the classical case, with a single shallow donor and the same parameters as above. Figure 7 gives the theoretical variation versus T of r_H for all three samples, and shows that taking $r_H=1$ leads to a considerable error, in particular at low T .¹⁶

The values quoted in Table I show that the introduction of a deep center with comparatively low concentration can account for a considerable reduction of the room- T Hall mobility (50% approximately for sample 1), with an increase in the free-electron concentration of comparable amplitude. A binding energy of 160 meV, extracted from $n_H(T)$, is found to be consistent with the experimental results of the samples showing a depressed

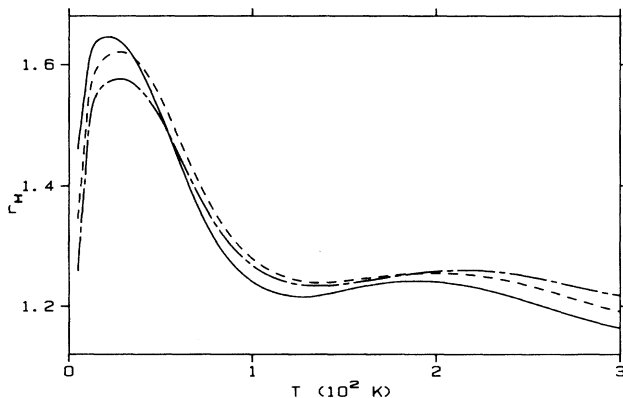


FIG. 7. r_H as computed from the parameters of Table I: continuous line, sample 1; dashed line, sample 2; dash-dot line, sample 3.

room- T mobility. Although the potential of Eq. (4) is unphysical, it has been shown to be equivalent, regarding scattering effects, to a potential of the form²⁰

$$V_1(r) = (V_0/r)\exp(-r/a), \quad (11)$$

which is the usual expression corresponding to an ionized impurity. For a shallow donor in InP, V_0 is approximately 6 meV, which, compared to the 160 meV of the deeper center, indicates more than one order-of-magnitude difference in scattering strength. Such a difference has been shown to be realistic when an adequate central core is added to the long range part of a single charge potential.²² Moreover, the values of a quoted in Table I are close to the usual screening lengths expected at high T for the doping levels being considered, and they decrease with increasing electron and impurity concentrations. This can be seen, for example, by using the Debye screening distance [$d = (\epsilon_0 \epsilon_s k_B T / q^2 n_c)^{1/2}$ in MKS units, ϵ_0 being the vacuum dielectric constant, k_B the Boltzmann constant, and q the charge of the electron], for which we obtain $d = 1881 \text{ \AA}$ for $n_c = 5 \times 10^{14} \text{ cm}^{-3}$ and $T = 300 \text{ K}$. If screening by fixed ionized impurities is added to the effect of the free electrons, as in the Brooks-Herring¹⁸ theory, the screening distance becomes $d = (\epsilon_0 \epsilon_s k_B T / q^2 n^*)^{1/2}$, with $n^* = n_c + N_D^+ (1 - N_D^+ / N_D)$, N_D and N_D^+ being, respectively, the concentrations of donor and ionized donor impurities. If N_D^+ is only slightly smaller than N_D , as expected at room T when most donor impurities are ionized, d is only slightly reduced by accounting for the ionized impurities.

Scattering by an acceptorlike isoelectronic center related to Carbon impurities has received considerable attention to explain a high- T mobility reduction often observed in early GaAs epilayers.^{1,2,23} Using the relaxation time

$$1/\tau_2 = 4(2)^{1/2} \pi^2 N_L \hbar^2 E^{1/2} / 3m^*{}^{3/2} E_L, \quad (12)$$

where E_L is an energy parameter associated with the scattering, E the energy of the electron, and N_L the concentration of centers, the corresponding mechanism could adequately explain the behavior of a set of moderately doped GaAs samples from 77 to 300 K with a single value of the parameter E_L , namely 95 meV². We investigated the possibility of such an effect. By assuming that all acceptors give rise to a localized center, attempts to reduce the theoretical room- T Hall mobility while keeping consistency with the experimental n_H led to unacceptably low values of E_L (of the order of 3 meV). Moreover, no combination of N_L and E_L can possibly explain the relative variation of μ_H between 77 and 300 K, these localized potentials reducing the mobility with approximately similar strength in the T range considered. The possibility of the presence of isoelectronic centers with a significant effect in the transport properties of InP epilayers has thus to be discarded.

In conclusion, we have shown that the presence of a deep-donor center explains both the reduction of the room- T Hall mobility and the additional electron excitation almost systematically observed for n -type InP epilayers.^{3–5} The binding energy of such a center is found to be 160 meV, its origin being still unclear. In addition, this complex does not appear to have any influence on

both the Hall mobility and the Hall electronic concentration at low T , when it is neutral, but it becomes a strong scatterer when ionized. A reassessment of the acoustical deformation potential of InP does not appear to be neces-

sary, the value $E_1 = 6.8$ meV being perfectly consistent with experiment when the deep center is accounted for. Scattering from a possible isoelectronic acceptorlike center linked to carbon impurities is also discarded.

-
- ¹G. B. Stringfellow and H. Kunzel, *J. Appl. Phys.* **51**, 3254 (1980).
- ²D. Chattopadhyay, *Phys. Rev. B* **23**, 2956 (1981).
- ³M. A. di Forte-Poisson, C. Brylinsky, and J. P. Duchemin, *Appl. Phys. Lett.* **46**, 476 (1985).
- ⁴D. A. Anderson and N. Apsley, *Semicond. Sci. Technol.* **1**, 187 (1986).
- ⁵C. H. Chen, M. Kitamura, R. M. Cohen, and G. B. Stringfellow, *Appl. Phys. Lett.* **49**, 963 (1986).
- ⁶Y. Takeda and A. Sasaki, *Solid-State Electron.* **27**, 1127 (1984).
- ⁷D. K. Hamilton, *Solid-State Electron.* **25**, 432 (1982).
- ⁸M. Benzaquen, D. Walsh, and J. Auclair, *Can. J. Phys.* **63**, 732 (1985).
- ⁹M. Benzaquen, K. Mazuruk, D. Walsh, C. Blaaw, and N. Puetz, *J. Cryst. Growth* **77**, 430 (1986).
- ¹⁰M. Benzaquen, K. Mazuruk, D. Walsh, A. J. Springthorpe, and C. Miner, *J. Electron. Mater.* **11**, 16 (1987).
- ¹¹D. L. Rode, *Low Field Electron Transport*, Vol. 10 of *Transport Phenomena*, edited by R. Willardson and A. Beer (Academic, New York, 1975).
- ¹²W. Walukiewicz, J. Lagowsky, L. Jastrzebski, M. Lichtensteiger, C. H. Gatos, and H. C. Gatos, *J. Appl. Phys.* **51**, 5 (1980).
- ¹³D. L. Camphausen, G. A. N. Connell, and W. Paul, *Phys. Rev. Lett.* **26**, 184 (1971).
- ¹⁴M. Benzaquen and D. Walsh, *Phys. Rev. B* **30**, 7287 (1984).
- ¹⁵M. Benzaquen, K. Mazuruk, D. Walsh, and M. A. di Forte-Poisson, *J. Phys. C* **18**, L1007 (1985).
- ¹⁶M. Benzaquen, D. Walsh, and K. Mazuruk, *Phys. Rev. B* **34**, 8947 (1986).
- ¹⁷M. Benzaquen, D. Walsh, K. Mazuruk, P. Weissfloch, N. Puetz, and C. Miner, *Can. J. Phys.* (to be published).
- ¹⁸H. Brooks, *Phys. Rev.* **83**, 879 (1951).
- ¹⁹A. R. Hutson, *J. Appl. Phys.* **32**, 2287 (1961).
- ²⁰N. Sclar, *Phys. Rev.* **104**, 1548 (1956).
- ²¹L. Schiff, *Quantum Mechanics*, 3rd ed. (McGraw-Hill, New York, 1968), p. 144.
- ²²A. A. Grinberg, *Fiz. Tekh. Poluprovodn.* **12**, 657 (1978) [*Sov. Phys.—Semicond.* **12**, 383 (1978)].
- ²³P. J. Dean, *J. Lumin.* **1/2**, 398 (1970).